EXPERIMENTAL INVESTIGATION OF WHIRL IN SELF-ACTING AIR-LUBRICATED JOURNAL BEARINGS

DAVID B. REYNOLDS

EXPERIMENTAL INVESTIGATION OF WHIRL IN SELF-ACTING AIR-LUBRICATED JOURNAL BEARINGS

BY

DAVID B. REYNOLDS

EXPERIMENTAL INVESTIGATION OF WHIRL IN SELF-ACTING AIR-LUBRICATED JOURNAL BEARINGS

BY

DAVID B. REYNOLDS
Lieutenant, United States Navy

Submitted in partial fulfillment of
the requirements for the degree of
MASTER OF SCIENCE
IN
MECHANICAL ENGINEERING
United States Naval Postgraduate School

Monterey, California
1962

NPS Archive
1962
Reynolds, D.

EXPERIMENTAL INVESTIGATION OF WHIRL IN SELF-ACTING AIR-LUBRICATED JOURNAL BEARINGS

****

BY

DAVID B. REYNOLDS

This work is accepted as fulfilling
the thesis requirement for the degree of
MASTER OF SCIENCE
IN
MECHANICAL ENGINEERING
from the
United States Naval Postgraduate School

ABSTRACT

Bearing characteristics influencing the threshold speed at which large-amplitude self-excited whirl occurs incomplete, air-lubricated journal bearings were experimentall investigated. Various combinations of rotors having clearance ratios, $\Psi = c/r$, ranging from 0.000268 to 0.002350 and symmetrical bearing assemblies having slenderness ratios, $L' = L/D$, ranging from 1/4 to 1 were tested.

By varying slenderness and clearance ratios and unit load, by opening or closing supply orifices, or by adding unbalance, the whirl threshold speed could be varied between zero and the limit set by the available power.

Experimental methods of identifying the cylindrical and conical modes of synchronous and self-excited whirl are described. The whirl hysteresis region and the nature of whirl at speeds above the threshold are examined. Three methods of avoiding large-amplitude self-excited whirl are discussed.

NOMENCLATURE

A	ratio of self-excited whirl amplitude to synchronous whirl amplitude
c	radial clearance, inches
D	bearing diameter, inches
e	eccentricity vector, connects the journal and bearing axes in a particular plane
I_p	polar moment of inertia, lb.-sec.^{2}-in.
I_t	translatory moment of inertia, lb.-sec.^{2}-in.
L	bearing length, inches
L'	L/D slenderness ratio
m	mass, lb.-sec.^{2}/in.
n	speed, rev./sec.
n_t	whirl threshold speed, rev./sec.
p_a	ambient pressure, lb./in.^{2}
r	bearing radius, inches
U	$r\omega$, relative surface velocity, in./sec.
W	bearing load, lbs.
W'	W/DLp_a, average bearing load in atmospheres
ϵ	e/c, eccentricity ratio, dimensionless
α	ratio of self-excited whirl component frequency to the synchronous component frequency, dimensionless
Λ	bearing number, $6\mu Ur/(c^2p_a)$, dimensionless
μ	film viscosity, lb.-sec./in.^{2}
ψ	c/r, clearance ratio, dimensionless
ω	rotational frequency, radians/second

CONTENTS

EXPERIMENTAL INVESTIGATION OF WHIRL IN SELF-ACTING AIR-LUBRICATED JOURNAL BEARINGS*

1. Introduction

As gas-lubricated bearings are more widely used, the lack of fundamental insight into certain characteristics of gas-bearing behavior becomes increasingly apparent. One such characteristic of self-acting gas-lubricated journal bearings is self-excited whirl, in which(if the journal is the rotating member) the journal axis orbits about an axis within the bearing with somewhat less than one-half the frequency of journal rotation. It is particularly important to understand the conditions affecting the threshold speed at which self-excited whirl occurs because this threshold usually limits safe operation. This paper concentrates on these conditions and presents experimental results obtained with a series of journal bearing assembles having two symmetrically located, approximately identical, bearings.

The equations of motion for a rotor in gas-lubricated journal bearings involve nonlinear time-dependent parameters which are functions of the eccentricity ratio ε ; clearance ratio ψ ;slenderness ratio L' ; mass m; moment of inertia,I; ambient pressure, p_a; film viscosity, μ ; relative surface

*This thesis represents a portion of the paper"Experimental Investigation of Whirl in Self-Acting Gas Lubricated Journal Bearings" by D.B. Reynolds and W.A. Gross, American Society of Lubrication Engineers 62AM 1A-4.

velocity, U ; the bearing length, L; and other geometric effects(such as unbalance, bearing location, and surface imperfections); and system considerations(such as drive effects, thrust bearing effects and resonances). The work reported here was limited to an investigation of the influence of bearing load, slenderness ratio, rotor mass, unbalance, and supply orifices on the threshold speed beyond which large-amplitude whirl occurs. The results are compared with those of previous investigations(1,2,3,4).

One of the two types of whirl--synchronous or self-excited---usually predominated, although in the threshold region, the amplitudes of both types of whirl may be approximately equal. Synchronous whirl is the passive response of the dynamic system to the drive force caused by unbalance; in this type of whirl, the orbiting speed is equal to the rotational speed of the journal. Self-excited whirl involves interaction of the lubrication film and the orbiting journal, and, unless metal-to-metal contact is made, the orbiting speed is slightly less than half the rotational speed. Both synchronous and self-excited whirl can occur in two modes; cylindrical and conical. In the cylindrical mode, the journal axis remains parallel to the bearing axis while orbiting. In the conical mode the journal axis generates a conical surface with the apex in the plane of the center of mass. Both the cylindrical and conical modes of whirl can be present concurrently, though separated by some phase angle and of different magnitudes. Usually the shirl path can be represented by a circle, an

ellipse, or a limacon, though in some cases the whirl path can be quite strange. See for example Fig. 1.

2. Description of apparatus

The bearing assembly, shown in Figs. 2 and 3(see also Fig. 3 in (5)), could be inclined to any angle. Since the only load applied in these tests was gravitational, the maximum load per bearing was one-half the rotor weight. To decrease axial constraints, only one thrust bearing was used (a contained step bearing with air-supply holes, which could be operated as a self-acting or as an inherently-compensated, externally-pressurized bearing).

Four assemblies with bearings having different slenderness ratio , but equal midplane spacings, were used. Each bearing had in its midplane sixteen equally spaced 0.020-inch orifices which were connected to a common air supply groove. Brass plugs and "O" rings, as shown in Fig. 3, were used to plug the orifices in some of the tests. Five rotors with different clearance ratios and masses were used. Table 1 lists the dimensions of the rotors and bearings used. Four brass capacitor probes sensed journal motion at the outermost 1/4inch rotors.

For the purposes of these tests, the rotors were driven by an impulse turbine composed of sixteen buckets cut into each rotor. Since two jets directed oppositely, 180°apart, were used, the net radial force on the rotor from the turbine was virtually zero.

With the exception of one aluminum rotor, the rotors

and bearings were all machined from 52100 steel in such a manner that the bearing surface was contained between two imaginary cylindrical surfaces with radii differing by from 6 to 10 microinches. This tolerance included surface roughness, out-of-roundness, taper, and curvature. To minimize misalignment, the two journal bearings were machined into the same block.

The capacitor circuit was such that a change in capacitance would result in a change in voltage(6). The capacitors were connected in push-pull fashion so that the differential voltage in the horizontal and vertical direction was applied to the horizontal and vertical plates of an oscilloscope. A counter was triggered once per revolution as a dark non-reflecting spot passed in front of a transistor photomultiplier. This impulse was also used to intensify the trace on the oscilloscope, thus providing a reference mark, hereafter called the counter spot.

The ambient conditions during the tests were as follows :

Temperature:	$75 \leq \text{Temp} \leq 85$ F
Relative Humidity:	$40 \leq RH \leq 70\%$
Ambient Pressure:	$14.55 \leq p_a \leq 14.65$ psi
	(14.6 psi used in calculations)

3. Test Procedure

The capacitance probes and associated equipment were balanced and calibrated as follows: A rotor was installed and

manually moved so that first it rested flush against the top, and then against the bottom of the journal bearings. The output of the vertical probes was balanced and the gain of the oscilloscope adjusted so that, as the rotor was moved from these extreme positions, the oscilloscope spot would move from the top to the bottom of the unit circle. The same procedure was followed for horizontal motion. The balance was checked by supplying external pressure to the journal bearings to center the journal. Under these conditions the oscilloscope spot had to be centered. Finally, the journal was removed and again the balance checked to be certain that the spot would be in the center of the oscilloscope. The reproducibility of eccentricity-ratio-amplitude measurements obtained with this method of calibration was within $\pm$ 0.04. The principal sources of error were the manual movement of the rotor, and changes in capacitance due to movement of the connecting leads.

Since the principal aim was to investigate the effects of bearing load and of clearance and slenderness ratios on the threshold speed, no effort was made to measure the eccentricity ratio for given load, and bearing number was determined from charts published by Raimondi(7).

The rotor speed was determined with a counter which was accurate to one revolution per second. In order to obtain a more accurate ratio of the orbiting frequency to the rotational frequency of the rotor, a ten-second count was used until at least four consecutive counts agreed within two revolutions.

Then, with the vertical output from one set of the capacitor probes applied to the counter, the frequency of the rotor's vertical motion was similarly determined. Thus the whirl ratio was established with an estimated accuracy of 0.2% for the speed range investigated.

The rotor was started in the vertical position. When the rotor speed was great enough for self-acting operation, the rotor elevation was reduced to the desired angle. No effects of system resonances were observed.

During purely synchronous whirl, there was usually a small, nearly circular trace on the oscilloscope. The counter spot indicated the position of the journal axis when the reference mark on the rotor passed the reflecting light. During predominantly self-excited whirl, two spots appeared approximately 180 degrees apart on the oscilloscope. The slight deviation from 180 degrees was caused by the small synchronous component always present. Since the whirl frequency was usually somewhat less than half the rotational speed, successive counter spots lagged slightly behind the previous spots on the oscilloscope, causing the spots to appear to rotate around the trace.

Phase relationships can be determined in several ways. The most direct method is to display the capacitor output on a time base and compare it with known frequencies. The method used here was to supple the electrical signal representing the vertical motion of the rotor in one bearing to the vertical axis of an oscilloscope, and the signal representing the verticalmotion in the other bearing to the horizontal axis.

The trace then could be analyzed to determine if rotor motion was conical, cylindrical, or both.

There are numerous possibilities for defining the threshold above which self-excited whirl occurs. For example, it is possible that a small self-excited component with magnitude as little as one percent of the synchronous component may occur throughout the predominantly synchronous region. Furthermore, there exists a hysteresis region, described fully later, because of the tendency of the self-excited component, once established, to maintain a large amplitude at speeds below the threshold necessary to produce this type of whirl.

This investigation concentrated upon the conditions causing the self-excited whirl to exhibit large changes in amplitude with changes in speed. As defined here, the critical or threshold speed is the rotational speed at which, in the absence of external shocks, an increase of less than 3 revolutions per second causes the eccentricity ratio of the self-excited whirl component to increase from a magnitude of less than 0.1 to a magnitude greater than 0.2. With bearings having slenderness ratios of 1, 3/4, or 1/2, and increase of about 1/2 rps above the threshold speed was sufficient to cause such a change in whirl amplitude. In general, results were reproducible within 2 rps, although under some conditions, it was necessary to increase the rotor speed toward the threshold very slowly in order to obtain reproducible results. The method of determining threshold speeds is described later.

Early in the experimental program, dirt particles caused a

failure in a test of the rotor with clearance ratio $\Psi = .268(10)^{-3}$ in the bearings with slenderness ratio $L' = 1$. For this reason, all of the rotor bearings given in Table 1 were not tested.

4. Experimental results

4.1. Effect of Orientation on the Threshold Speed

Threshold speeds differing by as much as 15 rps were obtained for equal elevation angles (and therefore, equal loading) depending upon the quadrant of the test fixture angle. It was also possible to vary the threshold speed by making minor changes in alignment of the thrust bearing. In fact, in the threshold region, it was possible to bring the system into and out of self-excited whirl simply by changing the alignment of the thrust bearing. The threshold speed was independent of thrust bearing supply pressures used.

The influence of orientation on threshold speed was probably due to such factors as thrust bearing misalignment, and the combination of relative radial translation and imperfections of the journal bearings, and axial translation of the rotor. When the data obtained for the threshold speed at a given rotor elevation angle from each side of the vertical were analyzed, it was noted that the average of these values was reproducible within 2 rps regardless of the thrust bearing conditions. It is this average threshold speed which is given in Table 2 and used in the figures.

4.2 Effect of Bearing Load on the Threshold Speed

The rotors were well enough balanced that the amplitudes of the synchronous whirl components of the eccentricity ratios were less than 0.1. When there was no measurable self-excited whirl, the position of the journal, for any rotor-bearing combination, was therefore determined almost entirely by the rotor weight. Since the unit loading (load per unit projected area, $W' = W/(DLP_a)$, expressed in atmospheres) was always less than 1/10 atm, the effect of compressibility was comparatively slight except at large eccentricity ratios. As a consequence, these tests, although involving air as a lubricant, could be used for confirmation of predictions based on the assumption that the lubricating film was incompressible. Increasing speed caused the eccentricity ratio to decrease until a threshold, at which the whirl amplitude grew rapidly, was reached. Until this point, the gravity loading resulted in an eccentricity ratio large enough so that the syschronous whirl paths did not go around the bearing center.

Figures 4 and 5 show the threshold speed, n_t, versus the unit loading. Note that in each case there is a nearly linear relation between unit load and threshold speed. This indicated that self-excited whirl would develop only after a threshold eccentricity ratio, which was nearly constant for each configuration, had been reached. Recall that the average bearing load supported by an incompressible film can be expressed as a product of the bearing number, $\Lambda = 6\mu Ur/(c^2 p_a)$, and a function of the eccentricity ratio. Since the bearing

number is directly proportional to the rotational speed, it is seen that, when the film is effectively incompressible, the threshold eccentricity ratio is constant for a particular configuration. It is unwise to attempt to apply these results when compressibility effects are significant.

4.3. Effect of Orifices on the Threshold Speed

Tests were run with the supply orifices closed and with the orifices open to the atmosphere. When the lubricant was permitted to flow in or out through the open orifices, the load capacity of the bearings was reduced. To support the load, with the orifices open, therefore, the eccentricity ratio was greater by as much as a factor of two for a given speed. As a consequence, the threshold speed was always higher, and in some cases, even doubled, when the orifices were open. In general, the smaller the clearance ratio, the greater the effect of open orifices on threshold speed. This is the only characteristic of whirl which was observed to be influenced by opening or closing the orifices . Table 2 shows comparative data for threshold speeds with orifices open and closed at the same unit loading.

4.4. Effect of Slenderness Ratio on the Threshold Speed

As can be observed from Fig. 6, decreasing the slenderness ratio tended to increase the critical speed for clearance ratios greater than $\Psi = 1.066(10)^{-3}$, and to decrease the threshold speed for smaller clearance ratios. With a unit load of 0.034 atm and orifices closed, changing the slender-

ness ratio from $L' = 3/4$ to $L' = 1/4$ increased the threshold speed 49% for $\Psi = 2.350(10)^{-3}$, and decreased it 25% for $\Psi = .568(10)^{-3}$. Increasing the slenderness ratio also tended to decrease the eccentricity ratio at which self-excited whirl occurred for a given clearance ratio, as shown in Fig. 7. It should be noted that the threshold eccentricity ratio varied from .1 to .9 depending on the slenderness and clearance ratios.

4.5 Effect of Clearance Ratio on the Threshold Speed

The tests indicated that, for any configuration, there may be a clearance ratio which will result in the lowest threshold speed. This is evident in Fig. 8; for example, with $L' = 3/4$, the lowest threshold speed occurred for $\Psi = 1.066(10)^{-3}$, larger values occurring for $\Psi = .568(10)^{-3}$ and $2.350(10)^{-3}$. These figures indicate that the clearance ratio at which the threshold speed is minimum is highly sensitive to the slenderness ratio. Ingeneral, at small clearance ratios, the effect of decreasing the slenderness ratio was to lower significantly the clearance ratio for the minimum threshold speed. The shape of the curve in Fig. 8 for $L' = 3/4$ is similar to that predicted (4) for $L' = 2$.

If the curves for threshold eccentricity ratio versus clearance ratio, shown in Fig. 9, are extrapolated to $\varepsilon = 0$, (dotted lines) we see that there appears to exist a clearance ratio below which a threshold eccentricity ratio does not exist. It can also be seen that increasing the slenderness ratio increases the value of the clearance ratio below which

no threshold eccentricity ratio can exist. If these extrapolations are valid, it appears that a combination of a sufficiently small clearance ratio and a sufficiently large slenderness ratio would result in a complete self-acting journal bearing which would not exhibit self-excited whirl.

It was observed that the smaller the clearance ratio, the smaller the calculated threshold eccentricity ratio. In fact, self-excited whirl could be prevented in bearings with very small clearance ratios by light loading, so that the threshold eccentricity ratio would never by reached.

A rotor with clearance ratio $\Psi = .268(10)^{-3}$ was operated in bearings with slenderness ratio 1 and orifices open at average loads from 0 to 0.022atm and at speeds up to 900 rps with no detectable self-excited whirl. Under no-load conditions, a small synchronous-whirl component was present with an eccentricity ratio magnitude of about 0.01 at 300 rps, increasing to 0.05 at 800 rps. At 900 rps, some dirt particles caused a failure and prevented further tests with this rotor and bearing.

4.6. Effect of Rotor Mass on the Threshold Speed

An aluminum rotor with $\Psi = 2.350(10)^{-3}$ and mass equal to 18.5% of the steel rotor with the same clearance ratio was tested. The results indicated that, at the same unit loads, there was no significant difference between the threshold speeds of the aluminum and steel rotors.

4.7. Effect of Unbalance

The tests previously described indicated that large-amplitude self-excited whirl cannot exist if the magnitude of

the eccentricity ratio is kept above a certain critical level. It seemed possible that the eccentricity ratio could be kept above the threshold value by centrifugal loading due to unbalance. This method was tested by adding 0.00226 in.-lb. of unbalance to the rotor with $\Psi = 2.350(10)^{-3}$ operating vertically in bearings with $L' = 1/2$. The otherwise unloaded rotor exhibited self-excited whirl at speeds below 32 rps. At this speed, the magnitude of the eccentricity ratio (0.8) was approximately that of the average threshold eccentricity ratio previously determined (0.74). There was no large-amplitude self-excited whirl above 32 rps, although the synchronous component grew with increasing speed.

This method of tuning a rotor to prevent self-excited whirl is likely to be of greatest value for small clearance ratios and low threshold eccentricity ratios. Only a small amount of unbalance would be necessary, and the synchronous whirl due to the unbalance would be acceptable for many situations.

4.8 Hysteresis Effect

Large-amplitude self-excited whirl, once established, usually does not subside until the rotational speed is decreased to a level below the threshold at which such whirl first occurred. This tendency of the whirl to persist below the threshold is called the hysteresis effect. Within the hysteresis region, it is possible to jar the assembly either into or out of large amplitude self-excited whirl. A small self-excited whirl component can be recognized at form 1 to 10 rps below the hysteresis region. The amplitude of this self-

excited eccentricity ratio component was observed to be from 0.1 to 1 times the synchronous component, which was itself always less than 0.1. In this sub-hysteresis region, jolts gave rise to large amplitude self-excited whirl, which subsided rapidly.

Figure 10 illustrates the size of the hysteresis region as a function of unit load for a particular rotor-bearing combination. In all cases, the speed change necessary for the self-excited whirl component to grow a specified amount appeared to be the same as that required for it to fall the same amount although the speeds were different. The extent of the hysteresis region may be due predominantly to squeeze film(damping) effects. It appeared that the extent of the hysteresis region decreased and the resistance to jolts increased with decreasing clearance ratio. Since the squeeze film effect is roughly proportional to the inverse cube of the minimum film thickness, the damping increases with decreasing clearance ratio(5). The damping resuling from decreased clearance ratio may explain the results achieved with $L' = 1/2$, orifices open and a constant load. Under these conditions, the rotor with $\Psi = 2.350(10)^{-3}$ could be jolted into large amplitude self-excited whirl at speeds as much as 20 rps below the threshold, whereas the rotor with $\Psi = .568(10)^{-3}$ could not be jarred into sustained self-excited whirl at speeds 3 rps below the threshold.

External vibrations had no noticeable effect on the reproducibility of the threshold speed of the rotor-bearing combinations

tested, except for the combination $L' = 1/4$, $\Psi = 2.350(10)^{-3}$, which was extremely shock-sensitive. A light tap on the test fixture was sufficient to produce momentary large-amplitude self-excited whirl at speeds as much as 200 rps below the threshold. As a result, the reproducibility of data for this rotor-bearing combination was poor and threshold speeds obtained for the two rotor orientations varied as much as 230 rps from the mean with about 0.1 atm average loading. This variation decreased with decreased loading to about 5 rps at 0.034 atm. The eccentricity ratio at which large-amplitude self-excited whirl occurred was as high as 0.9 for an average loading of 0.03 atm and decreased to 0.8 at an average loading of 0.1 atm. It appears that, as the clearance ratio increases and the slenderness ratio decreases, the magnitude of the threshold eccentricity ratio approaches 1.

4.9 Whirl Shape and Growth

The speed change necessary to cause self-excited components to grow rapidly in amplitude was dependent upon both slenderness and clearance ratio. For example, rotor-bearing combinations with $L' = 1$, $3/4$, and $1/2$, and $\Psi = 2.350(10)^{-3}$, $.568(10)^{-3}$ and $1.066(10)^{-3}$ showed sudden increases in the self-excited component with small changes in rotor speed. The amplitude of the self-excited component of the eccentricity ratio for such combinations changed from nearly 0 to as high as 0.8 as the speed was changed from 1 rps below to 1 rps above the threshold speed. The change was much more gradual with the rotor-bearing combinations in which $L' = 1/4$, and $\Psi = 1.066(10)^{-3}$

and $.568(10)^{-3}$. In these cases, increases in rotor speed of as much as 20 rps were required to increase the magnitude of the self-excited eccentricity ratio component from a value less than 0.1 to a value greater than 0.6.

The large-amplitude self-excited whirl tended to have nearly constant amplitude, as shown in Fig. 11, in which the traces represent the paths of the rotor axis in the two capacitor probe planes. Self-excited whirl paths were, however, far from circular in some cases (see, for example, Figs. 1 and 12) which represent self-excited whirl paths for the rotor-bearing combinations having $L' = 1/4$ and $\Psi = 2.350(10)^{-3}$ and $\Psi = 1.066(10)^{-3}$ respectively.

In general, the self-excited whirl motion involved both cylindrical and conical whirl in which the apex of the surface generated by the orbiting rotor axis lay outside of the bearings, as can be seen in Fig. 11 or 14. Because of the phase relationship between orbiting components, we found it particularly useful to use the connections described earlier.

Figure 14 shows some drawings of traces obtained by means of such connections. In this figure, (A) shows the trace for cylindrical whirl, (B) for conical whirl, (C) for combined cylindrical and conical whirl, and (D) the trace for whirl in which the frequency of the conical mode is exactly two times the frequency of the cylindrical mode, but the amplitude of the cylindrical mode is twenty times greater than that of the conical mode. Figure 14 (C) was drawn for a 90 degree phase relation between cylindrical and conical modes. The inclination of the ellipse would be different with different phase angles.

When the modes are coupled, the component amplitudes are functions of time. A lemniscate, as shown in Fig. 14 (D) was observed to be steady in time for a limited speed range for the combination $L' = 3/4, \Psi = 2.350(10)^{-3}$. The corresponding motion of the axis in the bearings was nearly circular. In general, as the rotor speed was increased above the threshold, the cylindrical mode predominated. The rotor with clearance ratio $.530(10)^{-3}$ had strongly coupled cylindrical and conical modes, and the orbiting changed periodically from one mode to the other. The rotor with clearance ratio $1.066(10)^{-3}$ had weak coupling and some energy exchange between modes could be detected. There was no detectable coupling for the other configurations.

The thrust bearing had a considerable influence on the magnitude of the conical mode. Increasing the thrust pressure with the rotor seiling on the thrust bearing decreased the conical component. On the other hand, the conical component was increased with increasing pressure when the rotor was hung from the thrust bearing. This effect may be explained by the fact that, when the rotor was hung from the thrust bearing, it was supported by the Bernoulli effect, so that the dynamical connection between the rotor and the thrust bearing was equivalent to a soft spring. When the rotor was supported on top of the thrust bearing the film thichness between the two was much smaller and the stiffness greater, so that the wobbling due to the conical orbiting was inhibited.

It appeared that, for the same rotor mass and bearing load, smaller clearance ratios permitted the rotor to operate at speeds above the whirl threshold. Although in no case was

whirl carried to eccentricity ratios exceeding 0.95, speeds up to 10 times the threshold speed could be attained when the unit load was less than 0.01 atm. The rotors with $\Psi = 1.066(10)^{-3}$ and $.568(10)^{-3}$ could be safely spun at speeds up to two times the threshold speed for $W' = 0.04$. It should be emphasized that the large-amplitude self-excited whirl can be stable to excitations which are too small to cause metal-to-metal contact. Large excitations can, however, cause whirl of sufficient amplitude to knock the rotor into the bearing. The growth of the self-excited component was explosive when both the unit load and the clearance ratio were large. In fact, the rotor with $\Psi = 2.350(10)^{-3}$ could not be carried beyond the threshold speed for unit loads above 0.04 atm. It seems likely than the squeeze film effects, which increase as the clearance ratio decreases, add appreciably to the range of stable operation in the presence of large-amplitude self-excited whirl.

4.10 Whirl Frequency

In all of the cases investigated, the ratio of the self-excited whirl component frequency to the synchronous component frequency, χ, was between 0.486 and 0.500. Decreasing the clearance ratio resulted in larger values of this whirl ratio. For example, with $\Psi = 2.350(10)^{-3}$, the whirl ratio was $0.485 \leq \chi \leq 0.490$, while with $\Psi = 1.066(10)^{-3}$ and $\Psi = .568(10)^{-3}$, the whirl ratio was $0.495 \leq \chi \leq 1/2$. Increasing the rotor speed to four times the threshold speed had no noticeable effect on the whirl ratio of any of the rotors tested. Furthermore, the value of the whirl ratio never exceeded 1/2.

5. Summary and Conclusions

Several useful conclusions may be drawn from the experimental results reported here; they are, however, strictly applicable only to the symmetrical rotor-bearing assemblies investigated. It is well known that whirl in self-acting gas-lubricated journal bearings can be synchronous or self-excited, and can involve cylindrical or conical modes. This investigation demonstrated that both types of whirl, and both modes, can be present simultaneously. It is important to note that both synchronous and self-excited whirl can be uniformly asympototically stable to excitations which are not large enough to cause initial metal-to-metal contact. At speeds above the whirl threshold, large eccentricity ratios are required for stable operation; below the threshold speed, the stable region for well-balanced rotors extends to small eccentricity ratios.

The threshold speed beyond which large-amplitude self-excited whirl occurs is a function of eccentricity ratio, clearance ratio, slenderness ratio, bearing length or diameter, mass, moments of inertia, ambient pressure, viscosity, and other geometrical and system effects. This investigation centered upon the effects of slenderness ratio and clearance ratio on the threshold speed and upon the character of the whirl. Eccentricity ratio effects were observed and two rotors with the same clearance ratio, but different mass, were compared.

Three particularly important observations concern methods of avoiding large-amplitude self-excited whirl. In the first two methods, eccentricity ratios greater than the threshold

amplitude are provided by drilling holes in the bearing mid-plane to permit breathing to or from the atmosphere, and by unbalancing the rotor so that centrifugal force keeps the eccentricity ratio above the threshold value. Thirdly, sufficiently small clearance ratios coupled with sufficiently large slenderness ratios appeared to prevent large-amplitude self-excited whirl.

The experiments reported here confirm some previously published observations:

1. There appeared to be a clearance ratio, for given unit load and slenderness ratio, which gives a minimum $n_t(3,4)$.
2. The threshold speed varied almost linearly with unit load for each rotor-bearing combination. Since the film was in the near incompressible region, this corresponded to a nearly constant threshold eccentricity ratio(3).
3. The threshold eccentricity ratio increased with increasing clearance ratio (3).
4. Orifices, open to the atmosphere, influenced $n_t(3)$.
5. The growth in amplitude of the self-excited whirl component was greater with increasing speed when Ψ and W' were large(3).
6. A hysteresis zone existed (3).
7. The whirl ratio was nearly 1/2 ($0.485 \leq \chi \leq 1/2$) (5).
8. Ingeneral, whirl was composed of both synchronous and self-excited components, each with cylindrical and conical modes separated by phase angles(5).

The experiments contradicted some previously published results:

1. The absence of large amplitude self-excited whirl under no-load conditions depended upon L' and Ψ ; previous results predicted large-amplitude self-excited whirl at all speeds under no-load conditions (3).
2. When W' was constant, n_t depended upon both Ψ and L'. It did not always decrease with increasing L', as previously reported (3).
3. The threshold eccentricity ratio corresponding to the clearance ratio for minimum threshold speed was not necessarily the smallest threshold eccentricity ratio, as previously reported (4).

The experiments revealed some hitherto unreported results:

1. Large-amplitude self-excited whirl could be prevented by (a) unbalancing the rotor, or (b) decreasing the clearance ratio.
2. Self-excited whirl existed in which the whirl path did not enclose the bearing axis.
3. The speed could safely be taken up to ten times the threshold speed for low load conditions and appropriate L' and Ψ .
4. The modes of whirl could be coupled or uncoupled.
5. It appeared that the threshold eccentricity ratio could be anywhere between 0 and 1 depending on Ψ and L'.
6. The clearance ratio at which n_t was a minimum was especially sensitive to L'.

There are several possible explanations for the fact that no self-excited whirl occurred in certain configurations. It may have been because the increase in the threshold speed for rotors with small clearance ratios was greater than the speed to which the rotors could be driven. Alternatively, the critical eccentricity ratio may have been small enough that the small unbalance caused synchrouous whirl of larger amplitude. Finally it is possible that no self-excited whirl will exist for appropriate combinations of mass, moment of inertia, clearance ratio, and slenderness ratio.

ACKNOWLEDGMENT

The author gratefully acknowledges the construction of test apparatus by B. Beye and N. Vaccaro. Their attention to details and useful suggestions were major factors in this experimental program. Acknowledgment is also made to Dr. W. A. Gross without whose help this investigation would not have been possible.

REFERENCES

1. Wildmann, M., "Experiments on Gas Lubricated Journal Bearings;" ASME paper No. 56-LUB-8.

2. Whitley, S., and Betts, C., "Study of Gas-Lubricated, Hydrodynamic, Full Journal Bearings," Brit. J. Appl. Phys. 10, 455-463 (1959).

3. Sternlicht, B. and Winn, L.W., "On the Load Capacity and Stablilty of Rotors in Cylindrical Gas-Dynamic Journal Bearings," Tech. Rept. for ONR, Contract No. NONR 2844(00), Task No. NR 097-34, July 3, 1961.

4. Rentzepis, G. M., and Sternlicht, B., "On the Stability of Rotors in Cylindrical Journal Bearings," Tech. Rept. for ONR, Contract No. NONR 2844 (00), Task No. NR 097-348, May 15,1961.

5. Gross, W. A., "Investigation of Whirl in Externally Pressurrized Air-Lubricated Journal Bearings," ASME paper No. 61-LUB -1.

6. Gross, W. A., "Use of Capacity-Controlled rf Energized Ionization Transducer for Balancing Rotors," Rev. Sci. Instr.30, 522-23 (1959).

7. Raimondi, A.A., "A Numerical Solution for the Gas Lubricated Full Journal Bearing of Finite Length," ASLE Trans.4, 131-55 (1961)

TABLE 1
CHARACTERISTICS OF ROTORS AND BEARINGS TESTED

Rotor Characteristics					
Clearance Ratio**	0.002350	0.000568	0.000268	0.001066	0.002350 (aluminum)*
Length (in.)	3.50	3.50	3.50	3.50	3.50
Diameter at 68°F (in.) **	0.999655	1.001437	1.001737	1.000939	0.999655
Mass (10^3 lb-sec^2/in.)	1.725	1.67	1.67	1.67	0.319
Polar Moment of Inertia (10^4 lb-sec^2 - in.)	2.45	2.39	2.39	2.39	1.295
Transverse Moment of Inertia (10^3 lb-sec^2 - in.)	1.880	1.825	1.825	1.825	0.390

Bearing Characteristics				
Length (in.)	0.250	0.500	0.750	1.000
Slenderness Ratio (L/D)	1/4	1/2	3/4	1
Diameter at 68°F (in.) **	1.002005	1.002005	1.002005	1.002005
Orifice Diameter (in.)	0.020	0.020	0.020	0.020
Number of Orifices	16	16	16	16 (open or closed as noted)
Distance Between Bearing Centers (in.)	2.000	2.000	2.000	2.000

*All other rotors and bearings tested were made of steel.

** Rotor and Bearing diameters are accurate to $\pm$ 5 microinches; clearance ratios to $\pm$ 5 (10^{-6}).

TABLE 2

EFFECT OF ORIFICES ON THRESHOLD SPEED, (RPS)

($W' = 0.034$)

$10^3\psi$	$L' = 1$	$L' = 3/4$	$L' = 1/2$	$L' = 1/4$
		Orifice Holes Closed		
2.350		104	134	155
1.066		78	85	71
0.568		84	72	63
		Orifice Holes Open		
2.350	132	139	155	180
1.066	139	130	130	116
0.568		160	145	95
		Percentage of Increase Obtained by Opening Orifices		
2.350		33.6	15.7	16.9
1.066		66.7	53	63.5
0.568		90.5	101	50.7

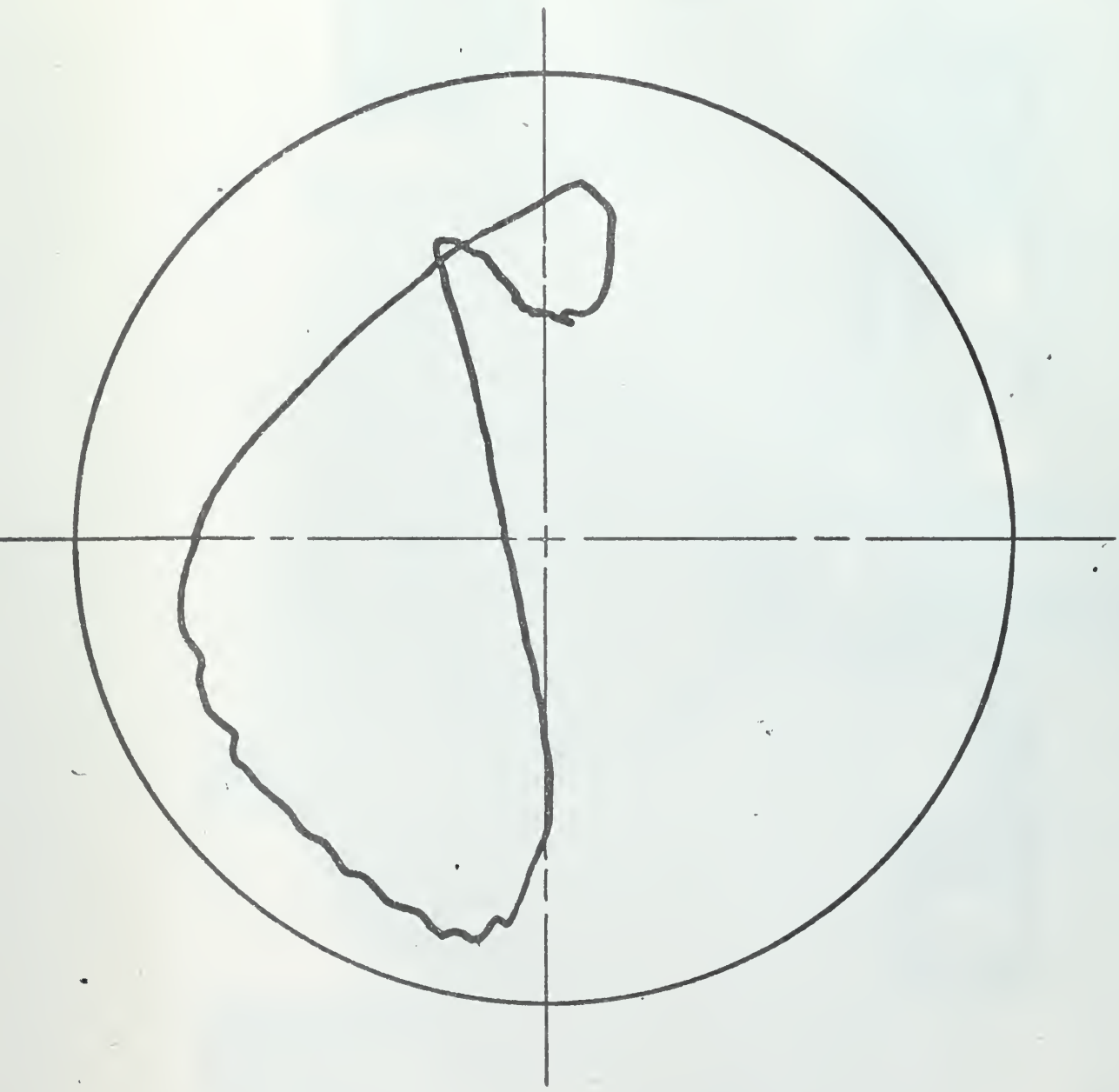

Fig. 1. Trace of Orbiting Journal with $\psi = 0.002350$, $L' = 1/4$, $n = 190$ rps, $W' = 0.0455$ atm

270
280
290
300
320
330
340
350
0
10
20
30
40
50
60
70
80
90
100
110

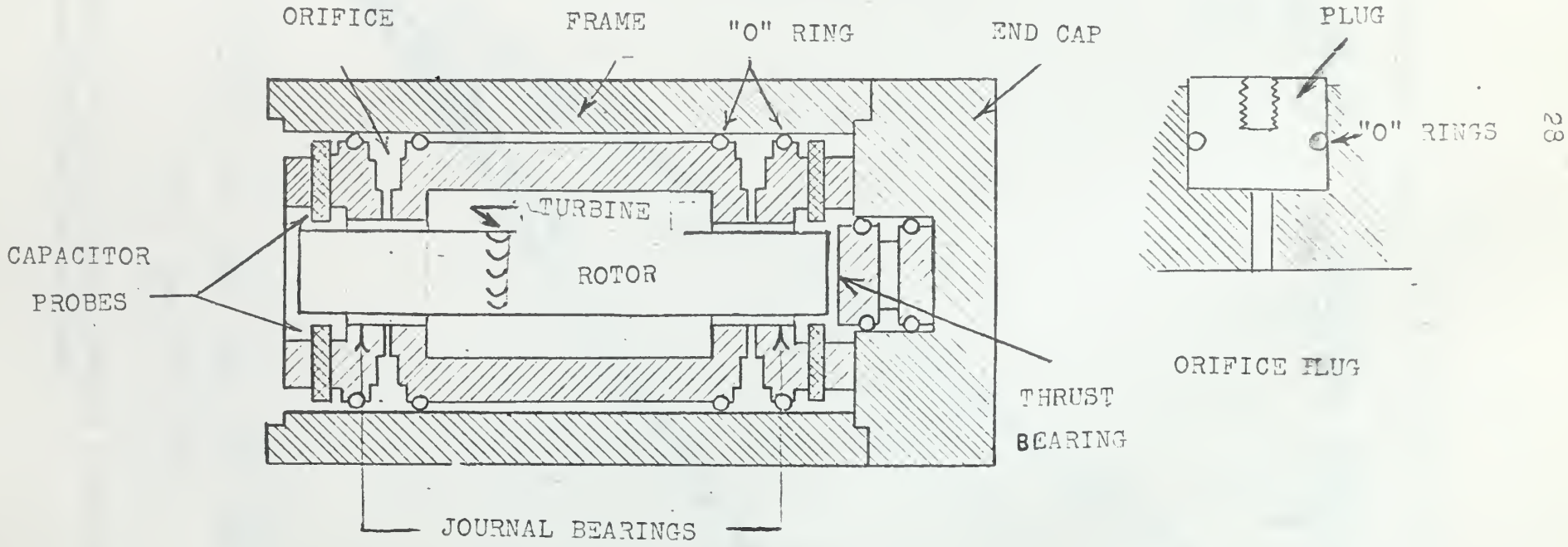

FIG. 3. Section of Bearing Assembly and Plugged Orifice

(not to scale)

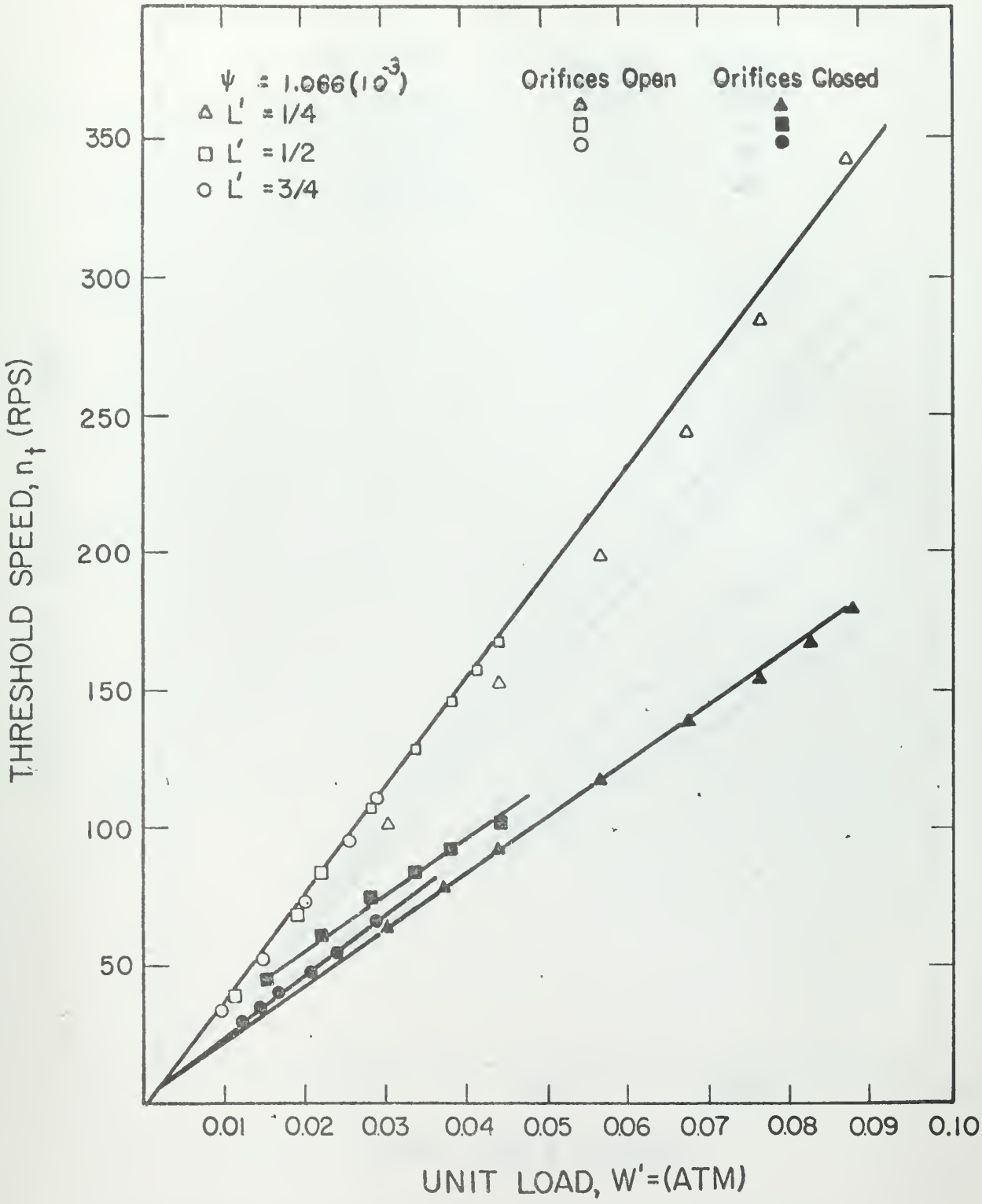

Fig. 4. Effect of Unit Load on Threshold Speed for Various Slenderness Ratios with Orifices Open and Closed

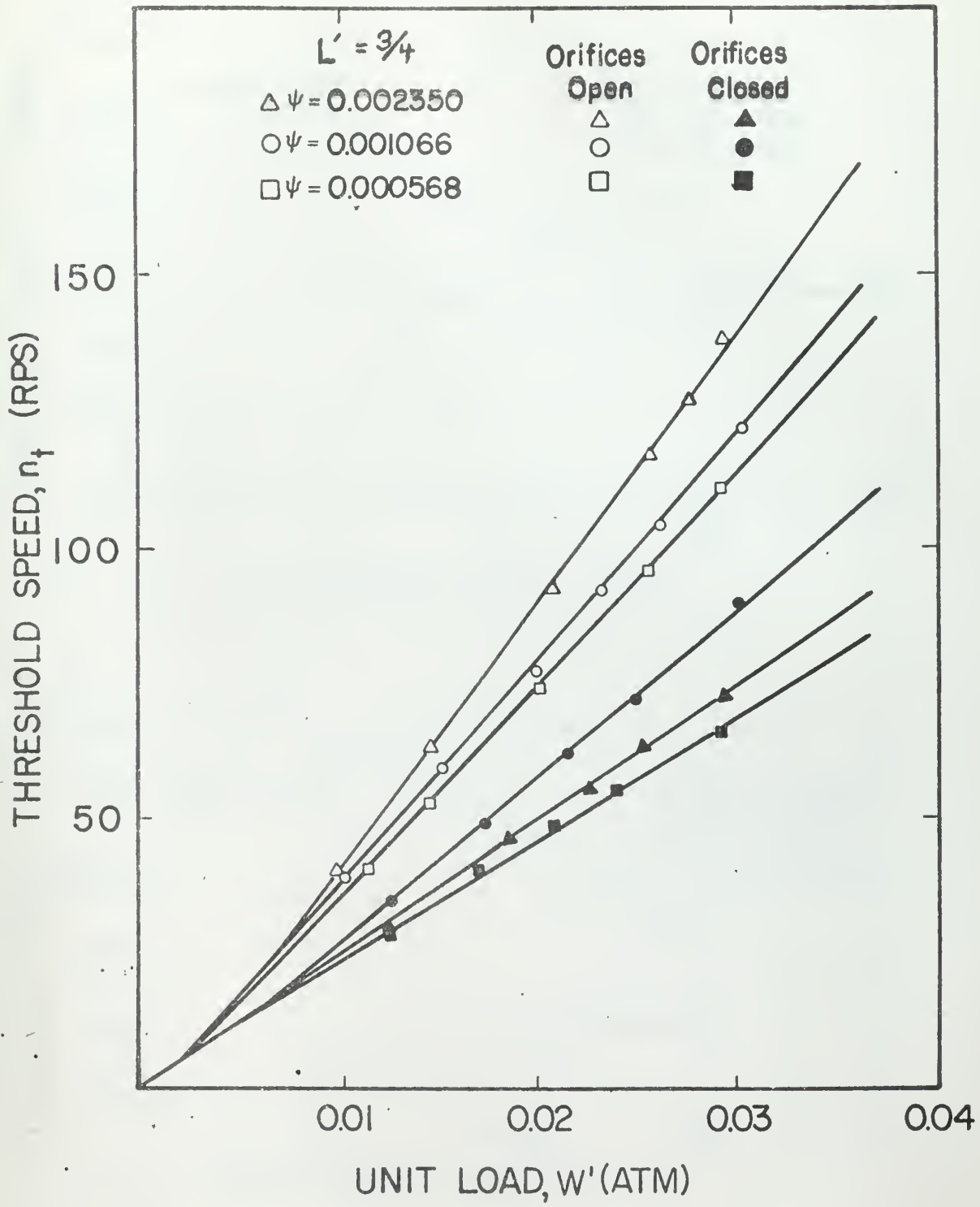

Fig. 5. Effect of Unit Load on Threshold Speed for Various Clearance Ratios with Orifices Open and Closed

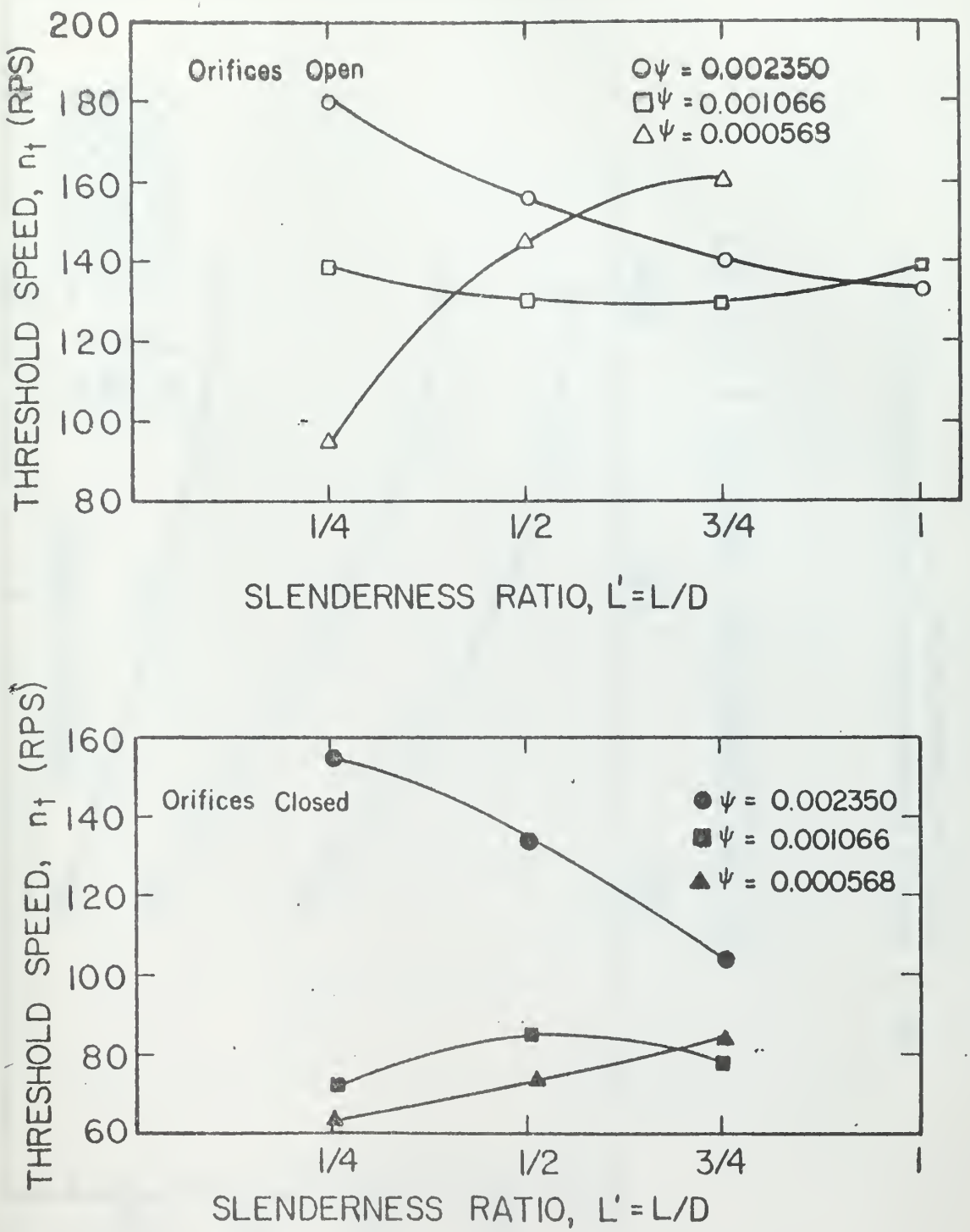

Fig. 6. Effect of Slenderness Ratio on Threshold Speed for Various Clearance Ratios with Orifices Open and Closed for W' = 0.034atm

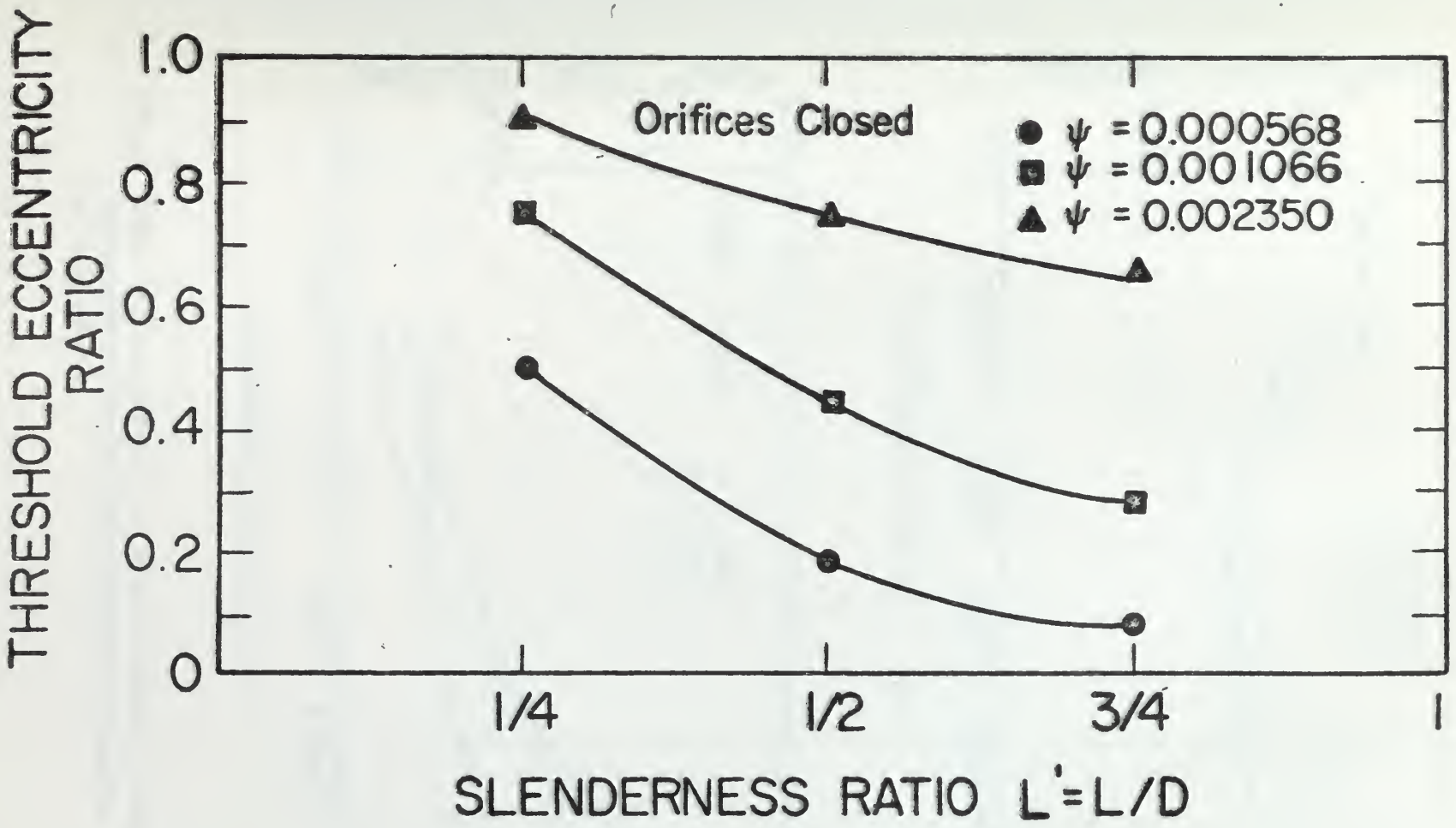

Fig. 7. Effect of Slenderness Ratio on Threshold Eccentricity Ratio for Various Clearance Ratios

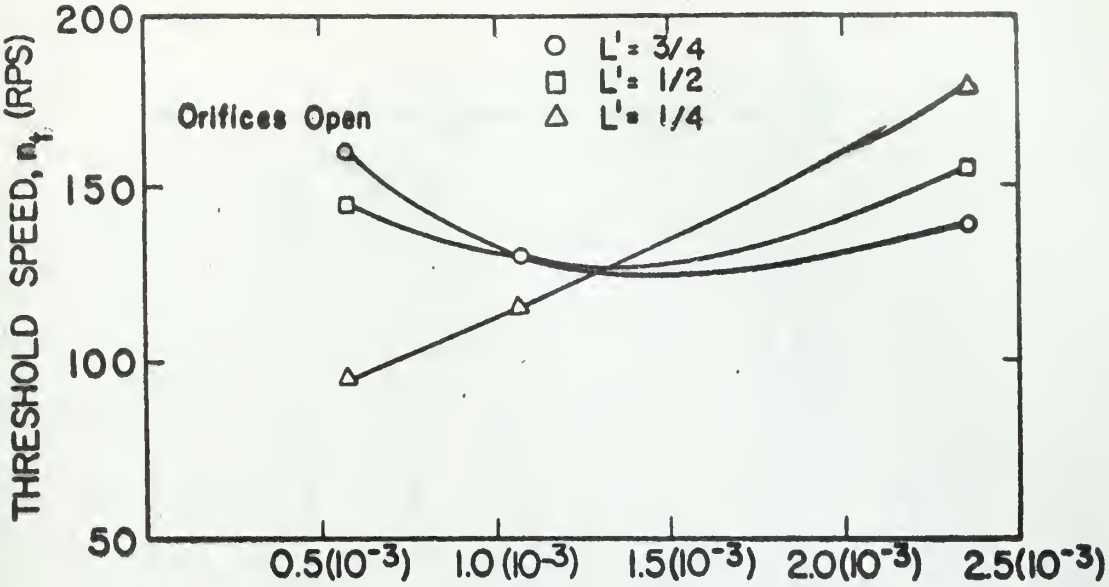

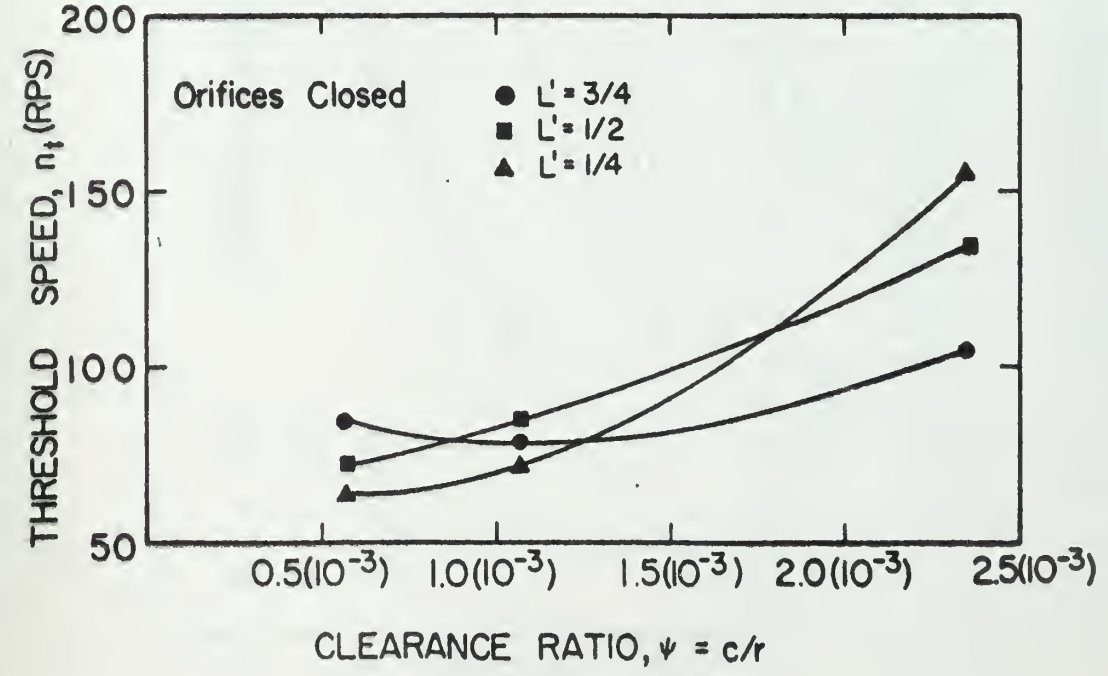

Fig. 8 Effect of Clearance Ratio on Threshold Speed for Various Slenderness Ratios with Orifices Open and Closed for W' = 0.034 atm

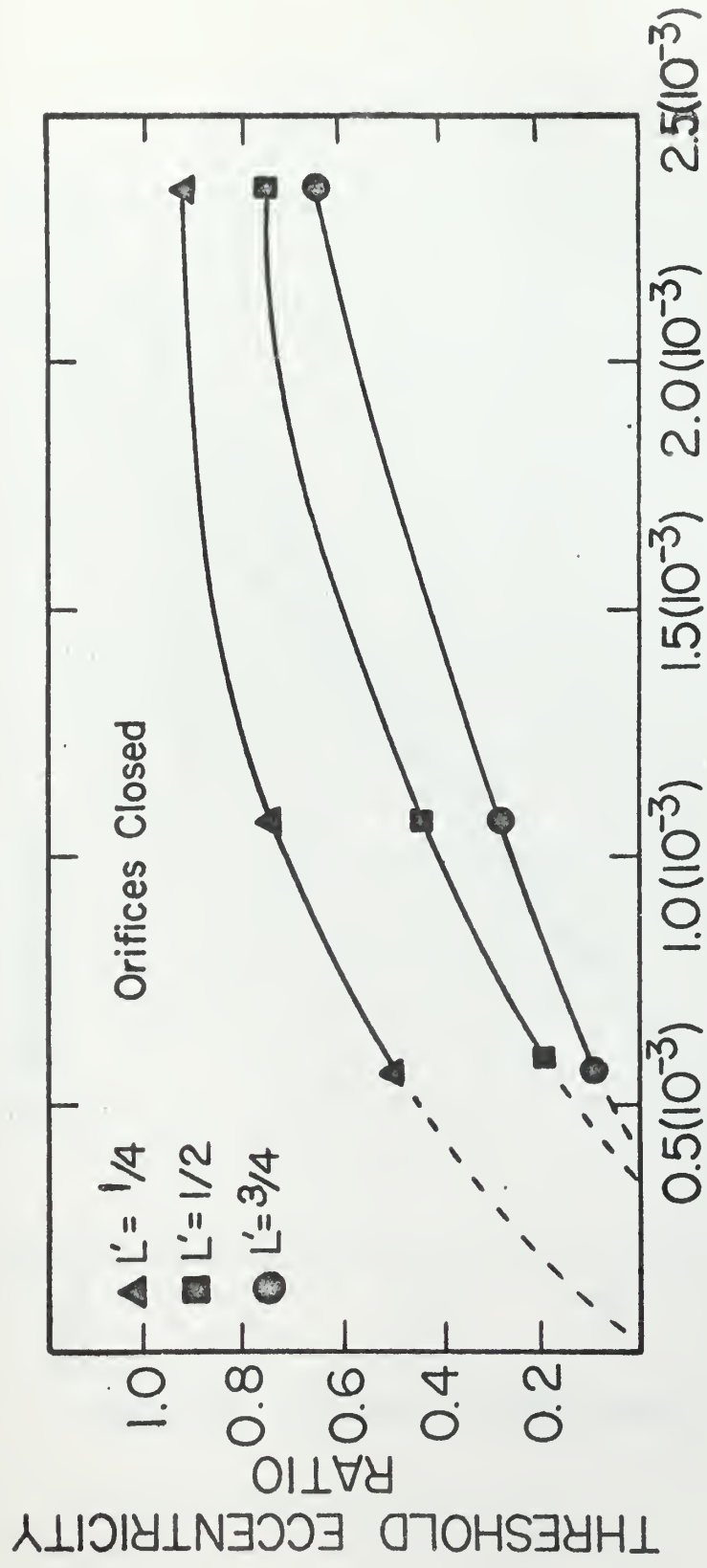

Fig. 9. Effect of Clearance Ratio on Threshold Eccentricity Ratio for Various Slenderness Ratios

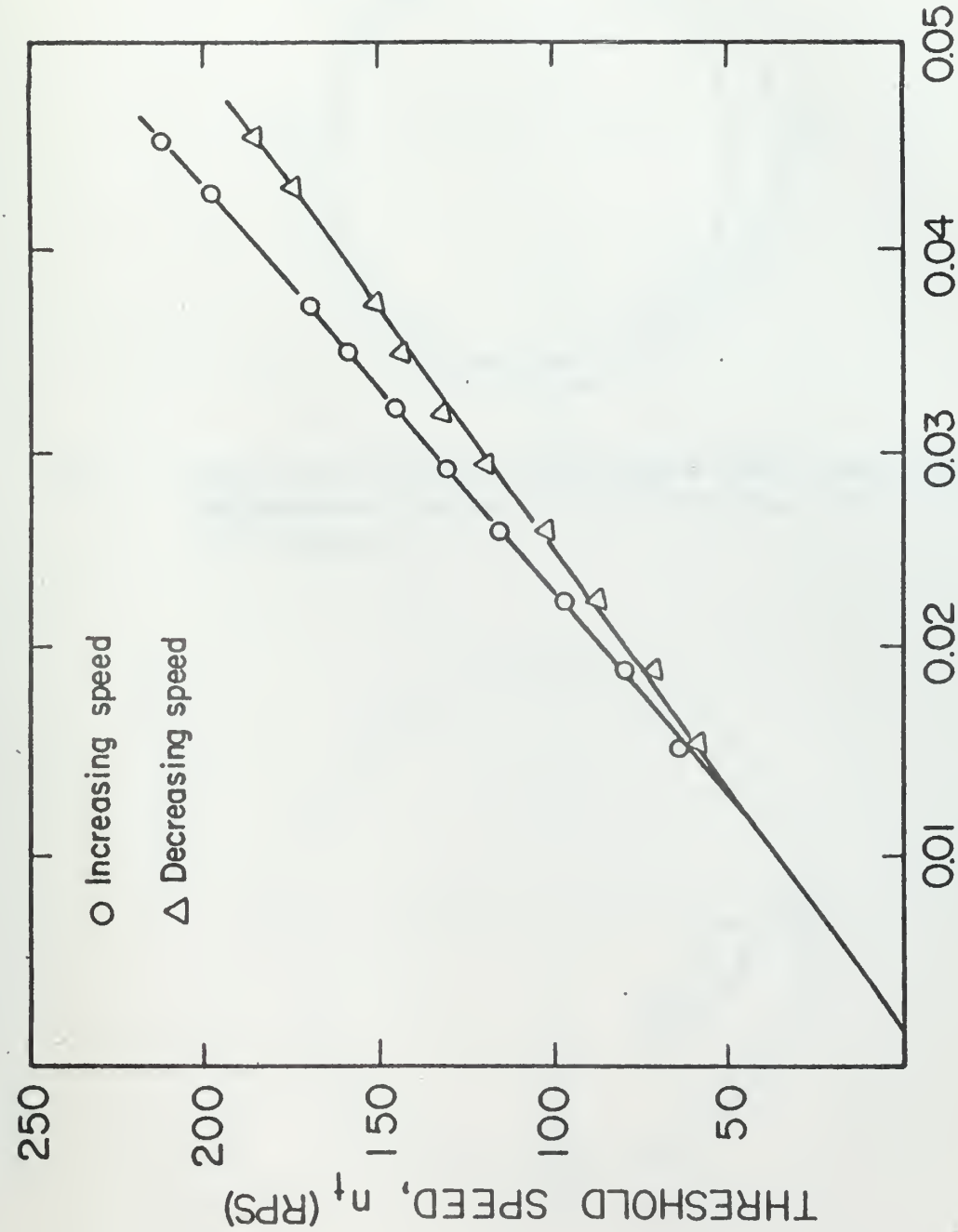

Fig. 10. Hysteresis Region of Threshold Speed for $\psi = 0.002350$, $L' = 1/2$

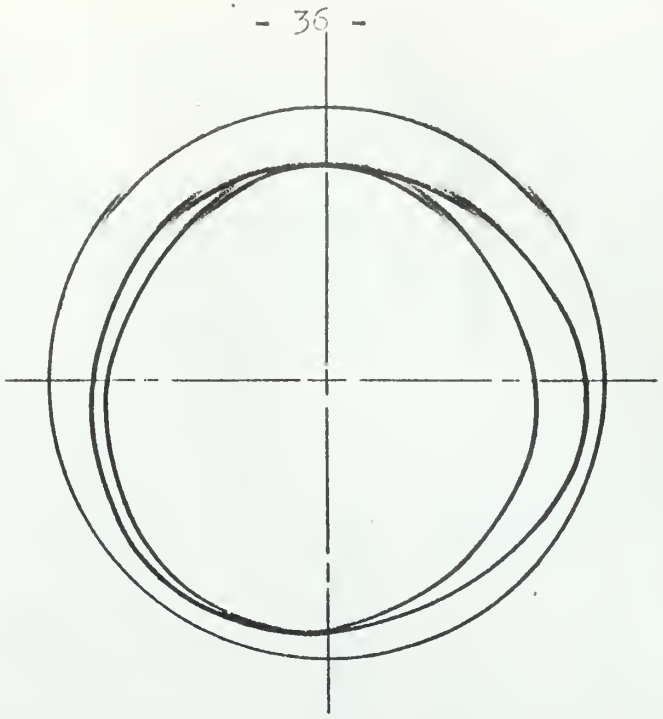

Fig. 11 Superposition of Traces of Orbiting Rotor Paths in Each of the Two Symmetrical Bearings, with $\psi = 0.001066$, $L' = 1$, $n = 120$ rps, $W' = 0.0221$ atm

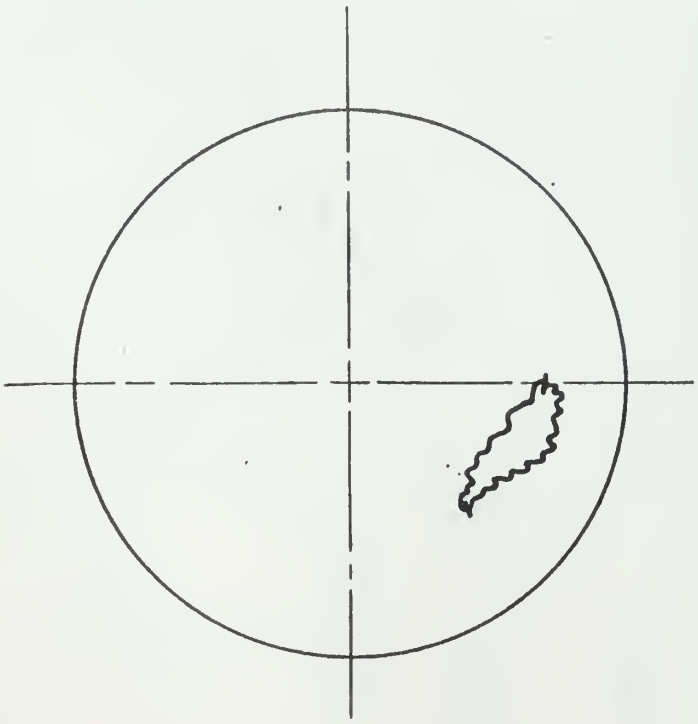

Fig. 12 Trace of Self-Excited Whirl for $\psi = 0.001066$, $W' = 0.065$, $n = 140$ rps, $L' = 1/4$ (orifices closed)

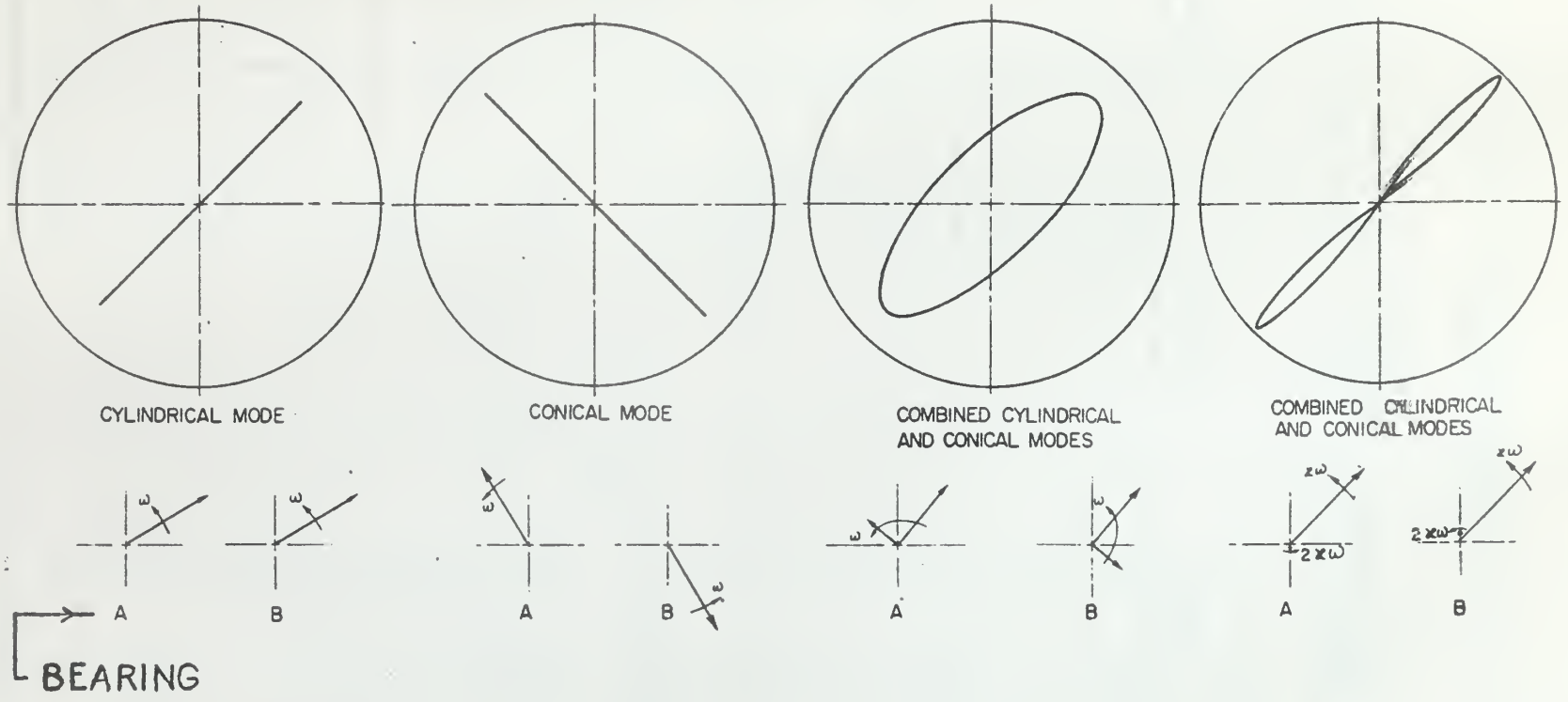

Fig. 13 Eccentricity Ratio Components and Corresponding Oscilloscope Traces for Purely Cylindrical, Purely Conical, and Combined Cylindrical and Conical Modes of Self-Excited Whirl

APPENDIX
EXPERIMENTAL DATA

ψ = 0.002350; Orifices Closed

L' = 3/4			
W/DL (psi)	$W' = W/(DLp_a)$	n_t(rps)	$\Lambda = 6\mu Ur/(c^2 p_a)$
0.441	0.0300	90	0.109
0.401	0.0273	82	0.0994
0.363	0.0247	74	0.0897
0.313	0.0213	62	0.0752
0.254	0.0173	49	0.0595
0.222	0.0151	42	0.0510
0.187	0.0127	35	0.0425
L' = 1/2			
0.662	0.0450	164	0.199
0.625	0.0425	156	0.189
0.576	0.0392	147	0.177
0.510	0.0347	134	0.163
0.427	0.0290	116	0.141
0.335	0.0228	93	0.113
0.228	0.0155	65	0.079
0.116	0.0079	30	0.0364

ψ = 0.002350; Orifices Closed (Continued)

$L' = 1/4$			
W/DL (psi)	$W' = W/(DLp_a)$	n_t (rps)	$\Lambda = 6\mu Ur/(c^2 p_a)$
1.32	0.0897	550	0.674
1.25	0.0850	500	0.606
1.09	0.0742	445	0.540
0.94	0.0640	382	0.464
0.762	0.0518	270	0.338
0.665	0.0452	230	0.279
0.562	0.0382	180	0.218
0.445	0.0303	128	0.155
0.345	0.0235	105	0.127
0.231	0.0157	72	0.0875

ψ = 0.001066; Orifices Closed

$L' = 3/4$			
W/DL (psi)	$W' = W/(DLp_a)$	n_t (rps)	$\Lambda = 6\mu Ur/(c^2 p_a)$
0.423	0.0288	66	0.390
0.352	0.0239	55	0.324
0.304	0.0207	48	0.283
0.247	0.0168	40	0.236
0.215	0.0146	35	0.207
0.182	0.0124	29	0.171
$L' = 1/2$			
0.642	0.0437	104	0.614
0.559	0.0380	93	0.549
0.494	0.0336	85	0.502
0.415	0.0282	74	0.486
0.322	0.0219	61	0.360
0.221	0.0150	45	0.266
0.167	0.0114	35	0.206
0.112	0.0076	25	0.147

ψ = 0.001066; Orifices Closed (Continued)

$L' = 1/4$			
W/DL (psi)	$W' = W/(DLp_a)$	n_t (rps)	$\Lambda = 6\mu Ur/(c^2 p_a)$
1.285	0.0874	180	1.06
1.21	0.0823	169	0.997
1.12	0.0762	155	0.915
.99	0.0673	140	0.825
0.83	0.0564	118	0.696
0.645	0.0439	93	0.549
0.545	0.0370	79	0.466
0.442	0.0300	64	0.378

ψ = 0.000568; Orifices Closed

L' = 3/4			
W/DL (psi)	$W' = W/(DLp_a)$	n_t (rps)	$\Lambda = 6\mu Ur/(c^2 p_a)$
0.428	0.0292	72	1.500
0.404	0.0275	67	1.393
0.372	0.0253	63	1.310
0.330	0.0224	55	1.144
0.276	0.0188	46	0.956
0.215	0.0146	35	0.727
0.182	0.0124	30	0.624
L' = 1/2			
0.642	0.0436	91	1.89
0.585	0.0398	81	1.685
0.539	0.0366	75	1.560
0.456	0.0310	64	1.33
0.370	0.0252	52	1.08
0.273	0.0186	38	0.79
0.167	0.0114	24	0.50

ψ = 0.000568; Orifices Closed (Continued)

$L' = 1/4$			
W/DL (psi)	$W' = W/(DLp_a)$	n_t (rps)	$\Lambda = 6\mu Ur/(c^2 p_a)$
1.285	0.0874	163	3.39
1.17	0.0795	148	3.08
1.055	0.0717	134	2.79
0.912	0.0620	113	2.35
0.740	0.0503	91	1.89
0.645	0.0439	79	1.64
0.545	0.0370	68	1.415
0.442	0.0300	54	1.123
0.334	0.0227	41	0.832

ψ = 0.002350; Orifices Open

L' = 1			
W/DL (psi)	$W' = W/(DLp_a)$	n_t(rps)	$\Lambda = 6\mu Ur/(c^2 p_a)$
0.333	0.0227	88	0.1065
0.235	0.0160	60	0.0726
0.166	0.0113	42	0.0510
0.114	0.0078	26	0.0315
L' = 3/4			
0.441	0.0300	122	0.148
0.416	0.0283	114	0.138
0.383	0.0260	104	0.125
0.339	0.0230	92	0.111
0.292	0.0198	77	0.0932
0.254	0.0173	68	0.0824
0.222	0.0151	59	0.0715
0.187	0.0127	49	0.0594
0.152	0.0103	39	0.0472

ψ = 0.002350; Orifices Open (Continued)

L' = 1/2			
W/DL(psi)	$W' = W/(DLp_a)$	n_t(rps)	$\Lambda = 6\mu Ur/(c^2 p_a)$
0.662	0.0457	212	0.257
0.625	0.0425	199	0.233
0.545	0.0371	170	0.206
0.510	0.0347	159	0.193
0.470	0.0320	145	0.176
0.427	0.0290	131	0.159
0.382	0.0260	115	0.140
0.332	0.0226	97	0.118
0.281	0.0191	80	0.0970
0.228	0.0155	64	0.0775
L' = 1/4			
1.325	0.0901	670	0.811
1.25	0.0850	650	0.788
1.09	0.0741	550	0.666
0.855	0.0582	365	0.443
0.645	0.0438	300	0.363
0.445	0.0303	160	0.194
0.345	0.0235	120	0.145
0.245	0.0167	85	0.103

ψ = 0.001066; Orifices Open

L' = 1			
W/DL (psi)	$W' = W/(DLp_a)$	n_t (rps)	$\Lambda = 6\mu Ur/(c^2 p_a)$
0.323	0.0220	87	0.554
0.303	0.0206	81	0.478
0.279	0.0190	75	0.442
0.246	0.0167	66	0.390
0.208	0.0142	53	0.313
0.161	0.0110	41	0.242
0.136	0.0093	33	0.195
0.110	0.0075	25	0.142
L' = 3/4			
0.428	0.0292	111	0.655
0.404	0.0275	104	0.614
0.372	0.0253	96	0.566
0.330	0.0225	84	0.495
0.293	0.0199	74	0.436
0.259	0.0176	64	0.378
0.215	0.0146	53	0.313
0.188	0.0128	46	0.272
0.168	0.0114	41	0.242
0.147	0.0100	34	0.201

ψ = 0.001066; Orifices Open (Continued)

L' = 1/2			
W/DL (psi)	$W' = W/(DLp_a)$	n_t(rps)	$\Lambda = 6\mu Ur/(c^2 p_a)$
0.642	0.0436	168	0.991
0.606	0.0412	158	0.932
0.559	0.0380	147	0.867
0.529	0.0360	139	0.820
0.494	0.0336	129	0.761
0.456	0.0310	119	0.702
0.415	0.0282	108	0.638
0.370	0.0251	96	0.566
0.322	0.0219	84	0.495
0.273	0.0186	70	0.413
0.221	0.0150	56	0.330
0.167	0.0113	40	0.236
0.112	0.0076	27	0.159
L' = 1/4			
1.270	0.0863	345	2.04
1.12	0.0762	286	1.69
0.988	0.0672	245	1.45
0.830	0.0565	198	1.17
0.645	0.0439	152	0.896
0.442	0.0300	101	0.596

ψ = 0.000568; Orifices Open

L' = 3/4			
W/DL (psi)	$W' = W/(DLp_a)$	n_t (rps)	$\Lambda = 6\mu Ur/(c^2 p_a)$
0.428	0.0291	138	2.86
0.404	0.0275	127	2.64
0.372	0.0253	117	2.44
0.304	0.0207	93	1.94
0.215	0.0146	63	1.310
0.147	0.0100	40	0.832
L' = 1/2			
0.642	0.0436	184	3.83
0.606	0.0413	175	3.64
0.559	0.0380	162	3.37
0.494	0.0336	145	3.02
0.456	0.0310	135	2.81
0.415	0.0282	121	2.52
0.370	0.0251	108	2.25
0.322	0.0219	95	1.98
0.273	0.0186	78	1.63
0.221	0.0150	63	1.31
0.167	0.0114	47	0.98

Ψ = 0.000568; Orifices Open (Continued)

L' = 1/4			
W/DL(psi)	$W' = W/(DLp_a)$	n_t(rps)	$\Lambda = 6\mu Ur/(c^2 p_a)$
1.285	0.0874	237	4.94
1.170	0.0795	217	4.12
0.988	0.0672	189	3.93
0.830	0.0565	162	3.37
0.645	0.0439	126	2.62
0.442	0.0300	80	1.66

Ψ = 0.002350; ORIFICES OPEN

	L' = 1/2	
W/DL (psi)	$W' = W/(DLp_a)$	lower n_t* (RPS)
0.662	0.0457	185
0.625	0.0425	174
0.545	0.0371	151
0.510	0.0347	143
0.470	0.0320	132
0.427	0.0290	118
0.382	0.0260	103
0.332	0.0226	88
0.281	0.0190	73

* Lowest rotor speed at which self-excited whirl will exist at given bearing load.